

Impacts of operating conditions on specific cake resistance in dead-end microfiltration process

Natsagdorj Khaliunaa¹, Wang Zhan^{1,2}, Xi Wang³, Tungalagtamir Bold^{4,*}

¹ Beijing Key Laboratory for Green Catalysis and Separation, School of Chemistry and Chemical Engineering, Beijing University of Technology, Beijing, P.R. China

² College of Environmental Science and Engineering, Tongji University, Shanghai, P.R. China

³ Faculty of Humanities and Social Sciences, Macao Polytechnic University, Macao, PR China

⁴ Laboratory of Fossil Fuel Processing, Department of Chemical Engineering, School of Applied Sciences, Mongolian University of Science and Technology, Ulaanbaatar, Mongolia

ARTICLE INFO: Received: 07 Dec, 2022; Accepted: 18 Jan, 2023

Abstract: In the present work, the fouling behavior and the corresponding specific cake resistance of polyethersulfone microfiltration membrane fouled by using different solutions (bovine serum albumin solution, sodium alginate solution, humic acid and activated sludge suspension) under different operating conditions, transmembrane pressure (*TMP*), concentration (*C*), stirred speed (ω) and temperature (*T*) were systematically investigated. The ensuing results showed that the proposed equation can be used to accurately calculate instantaneous specific cake resistance (α). The average specific cake resistance increased with increasing operating pressure, concentration, and stirred speed, while it decreased with increasing operating temperature. The average specific cake resistance of sodium alginate (SA) was larger and the sequence was SA>HA>BSA>AS.

Keywords: Specific cake resistance; fouling mechanism; microfiltration membrane;

INTRODUCTION

Water pollution and water scarcity, against the backdrop of explosive world population growth, have become a critical problem of our time [1,2]. Today, membrane separation technology, the most widely used and the most common pressure driving membrane technology, has become instrumental in separating and purifying wastewater treatment [3]. However, the main obstacle to the microfiltration membrane filtration is the flux decline due to membrane fouling, which is the key and an unavoidable problem in the filtration process.

Membrane fouling in microfiltration is a very complicated process primarily caused by adsorption of particles, pore shrinkage (blockage) and deposition of particles on the membrane surface and concentration polarization [4,5,6]. Therefore, the characteristics of the cake, such as its thickness, porosity, compressibility and the specific cake resistance (SCR) play an important role. Among them, the SCR is the most important factor that revealed the physical characteristics of the cake, and its accurate knowledge is crucial for adequately designing and scaling-up of the practical membrane systems [7].

*corresponding author: botungalagtamir@must.edu.mn

<https://orcid.org/0000-0003-1469-6080>



The Author(s). 2022 Open access This article is distributed under the terms of the Creative Commons Attribution 4.0 International License (<https://creativecommons.org/licenses/by/4.0/>), which permits unrestricted use, distribution, and reproduction in any medium, provided you give appropriate credit to the original author(s) and the source, provide a link to the Creative Commons license, and indicate if changes were made.

In the past few decades, a lot of work on the membrane fouling mechanisms in MBR was done [8,9,10]. Among them, composite mechanism (pore clogging, pore blocking and cake filtration) was believed to be the predominant mechanism due to the wide particle size distribution [8,11,12]. Meanwhile, extracellular polymeric substances (EPSs), which consist of protein, hums and polysaccharide, were found to be the key membrane fouling substances in MBR [9,13,11,10] and many efforts have been made to figure out membrane fouling by using EPS model solution (BSA, HA and SA) [14–15].

For example, Hou et al. developed a triple-mechanism (pore blockage, pore constriction and cake filtration) model to describe the BSA fouling behavior in constant pressure dead-end filtration mode [16]. Hou et al. established a precise dual-mechanism (complete pore blocking and cake filtration) model to describe the fouling behavior for BSA solution [17]. In addition, Wu et al. proposed a triple-mechanism model to describe the flux decline for activated sludge suspension in MBR [18].

Table 1. The fouling mechanism for different feed

Foulants	Mechanism	Operating mode	Ref.
BSA	Complete pore blocking+cake filtration mode	Constant pressure dead-end	[19-21, 22]
	Pore blocking+pore constriction+cake filtration mode	Constant pressure dead-end	[20]
	Pore blocking+cake filtration mode	Constant pressure dead-end	[23]
HA	Pore blocking + pore constriction + cake filtration mode	Constant pressure dead-end	[24]
SA	Standard pore blocking +cake filtration mode	Constant flux cross-flow	[25]
Activated sludge	Pore blocking +pore constriction+cake filtration mode	Constant pressure dead-end	[26]

Specific cake resistance is dependent on numerous factors, such as operating conditions (trans-membrane pressure [TMP], concentration, and temperature) [27,28], particle diameter, particle shape, cake porosity [29] and suspension properties, including pH [30-31] and ionic strength [32]. For example, the SCR increases with an increase in TMP [28]. Furthermore, the SCR also changes as the temperature varies. However, up to now, only few quantitative studies about the interactive effects of different operating conditions on the SCR have been found [33]. Hence it follows thsy up to now no solution has bene found as how to establish the relationship between specific cake resistance and operating conditions (trans-membrane pressure [TMP], concentration, stirrer speed, and temperature). The aim of this paper is to establish the relationship between specific cake resistance and operating conditions (trans-membrane pressure [TMP], concentration, stirrer speed, and temperature).

Theory

According to Darcy’s law [34], the flux in dead-end mode filtration can be expressed as follows.

$$J = \frac{dV}{Adt} = \frac{\Delta P}{\mu(R_t + R_m)} \tag{1}$$

Where J is the permeate flux of the membrane ($m^3 \cdot m^{-2} \cdot s^{-1}$); is the trans membrane pressure (Pa ;) R_m and R_t respectively are the intrinsic membrane resistance and the total fouling resistance(m^{-1}).

$$R_t = m\alpha = \frac{cV}{A} \alpha \tag{2}$$

where m is cake mass (kg/m^2); α is specific cake resistance (m/kg), C is feed concentration (kg/m^3), V is filtrate volume (m^3) and A is membrane filtration area (m^2).

Substitution from Eq.(2) into Eq.(1) gives the instantaneous specific cake resistance (α) as following:

$$\alpha = \frac{R_m A}{cV} \left(\frac{J_0 - J}{J} \right) = \frac{\Delta P A}{\mu J_0 c V} \left(\frac{J_0 - J}{J} \right) \quad (3)$$

where μ is viscosity (Pa·s) and J_0 is the pure water flux of the membrane ($m^3 \cdot m^{-2} \cdot s^{-1}$).

How to determine average specific cake resistance (SCR)

The SCR can be determined by using the following two methods.

1. The slope method

Based on cake filtration mechanism, if plotting t/V versus V [7] under constant TMP, the obtained slope value can be used to calculate the average SCR ($\bar{\alpha}$) by using the equation (4):

$$\frac{t}{V} = \frac{R_m \mu}{A_m \Delta P} + \bar{\alpha} \frac{\mu C}{2A_m^2 \Delta P} V \quad (4)$$

where t is filtration time (s), V is the total volume of permeate (m^3), A_m is the membrane area (m^2), and C is the concentration (g/L^{-1}), respectively.

2. The calculation method

The instantaneous specific cake resistance can be calculated by using Equation (3) and their average value can be calculated by using the following equation:

$$\bar{\alpha} = \frac{1}{n} \sum_{i=1}^n \alpha_i \quad (5)$$

MATERIALS AND METHODS

Polyethersulfone (PES) microfiltration (MF) membrane with nominal pore sizes of 0.1 μm from the Beijing Chemical Engineering University Liming Membrane Material Corporation was used as the filtration medium. Before each experiment, the membranes were soaked in deionized water for 24 hours to remove glycerin, which was used as a protectant in the membranes. The four kinds of feed suspensions/solutions were prepared as follows:

The preparation of humic acid (HA) solution: a stock HA solution (2g/L) was prepared as follows. Firstly, 2 g of HA was dissolved in 1 L of NaOH solution (pH=12). Next, the solution was stirred for 24 hours, and the pH of the solution was adjusted to 7.0 using 1mol/L HCl. Then, the stock solution was

The membrane flux was calculated by using Eq. (6) and the resistances (the virgin membrane resistance (R_0), the cake resistance (R_c), and complete blocking resistance (R_b)) were calculated respectively by using the method as described in the report [17].

$$J = \frac{J_0 \left((1-K) \exp\left(\frac{-K_b}{K_c J_0^2} \left((1+2K_c J_0^2 t)^{\frac{1}{2}} - 1 \right) \right) + K \right)}{(1+2K_c J_0^2 t)^{\frac{1}{2}}} \quad (6)$$

Determination of the sum of squared deviations (SSD)

The sum of squared deviations (SSD), and the relative deviation (σ) between experimental data and model predictions were used to evaluate the accuracy of the models [20], which was calculated by using the following equations.

$$SSD = \frac{\left(\sum_m^N (J_m - \hat{J}_m)^2 \right)}{N} \quad (7)$$

$$\sigma = \frac{\left(\sum_m^N \sqrt{(J_m - \hat{J}_m)^2 / J_m^2} \right)}{N} \times 100\% \quad (8)$$

where J_m and \hat{J}_m was the experimental and predictive permeation flux at filtration time m , respectively. N was the sample number.

stored at 4°C in the dark. A HA concentration of 5 mg/L was chosen to simulate the organic matter content in surface water (Sutskover-Gutman et al., 2010, Tian et al., 2013) and was prepared by diluting the stock solution with Milli-Q water [35].

The preparation of sodium alginate (SA) solution: the stock solutions (1g/L) of SA were prepared by dissolving 1 g of SA into 1 L ultrapure water, followed by stirring for 24 h. The stock solution was stored at 4°C in the dark [36].

The preparation of activity sludge (AS) solution: the feed solution (raw wastewater) was obtained from the storage tank of domestic sewage with qualities shown in Table 2. The operating parameters for the bioreactor system, such as the mixed liquor suspended solid

(MLSS), temperature (T), dissolved oxygen (DO), pH and hydraulic retention time (HRT),

are shown in Table 3. No sludge was discharged during the operation or the test period.

Table 2. The qualities of raw wastewater

COD (mg/L)	NH3-N (mg/L)	TOC (mg/L)	pH	Turbidity /NTU
180.6-225.8	45.9-73.6	86.5-115.5	7.5-8.0	20-26

The main parameters of the feed suspension into the membrane cell used in the experiments were total oxygen content (TOC) (33.5-38.4 mg/L) NH3-N (9.7-10.75 mg/L) and chemical oxygen demand (COD) (48.2-52.6 mg/L). The mixer liquor suspended solids

(MLSS) concentration was measured by weighing a dried sample and pH was measured with a pHS-3C acidity meter. The COD and NH3-N of the membrane influent and effluent were measured by adopting the Chinese SEPA standard methods [37].

Table 3. Operating parameters of bioreactor

MLSS (g L ⁻¹)	T (oC)	DO (mg L ⁻¹)	pH	HRT (h)
2.7	20	4.0	7.5-8.0	18

The preparation of Bovine serum albumin (BSA) solution: BSA solutions were prepared by dissolving BSA powder in phosphate buffer saline (PBS) solution (8.0 g NaCl, 0.2 g KCl, 0.27 g KH₂PO₄ and 1.42 g Na₂HPO₄ in 1 L DI-water, pH=7.4) to obtain 1 g/L homo-geneous BSA-PBS solution. After which the desired solution was prepared by diluting PBS solution to a certain level of concentration and generally used within 12 hours [17]. All experiments were conducted in a dead-end filtration cell with an effective membrane area of 28.0 cm² and a working volume of 250 ml.

Operating Conditions

Tests were conducted at a temperature of 20°C, concentration of 1.22g/L for AS suspension, 0.1g/L for SA solution, 5mg/L for HA solution and 0.05g/L for BSA solution by using 0.1 μm PES membrane in the pressure range of 0.1MPa to 0.2MPa.

Experiments were conducted at a temperature of 20°C, transmembrane pressure of 0.1MPa, at concentrations of 1.22, 4 and 7g/L for AS, 0.04, 0.06, 0.08 and 0.1g/L for SA,

2, 5, 8 and 10 mg/L for HA and 0.02,0.05 and 0.07g/L for BSA by using 0.1 μm PES membrane.

Experiments were conducted at a temperature of 20°C, transmembrane pressure of 0.1MPa, at concentrations of 0.4 g/L for AS, 0.1g/L for SA, 10 mg/L for HA, 0.05 g/L for BSA and stirred speed in the range of 200 rpm to 1000 rpm by using 0.1 μm PES membrane.

Experiments were conducted at a temperature of 20°C, transmembrane pressure of 0.1MPa, at concentrations of 1.22 g/L for AS, 0.1g/L for SA, 5mg/L for HA , 0.1 g/L for BSA and temperature in the range of 30°C , 40°C to 50°C by using 0.1 μm PES membrane.

Experimental set-up

The fouling tests were conducted in a constant pressure ultrafiltration dead-end stirred cell with an effective membrane area of 28.0 cm² (Figure 1). The UF cell consists of a cylindrical vessel, equipped with porous support on which the membrane has been placed.

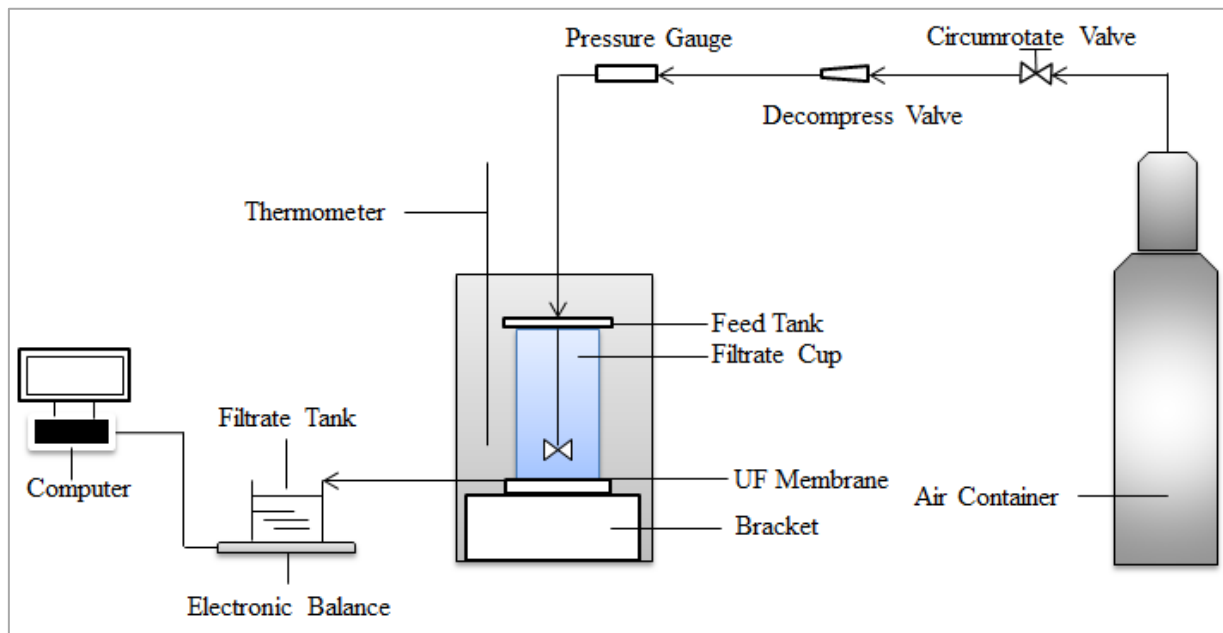


Figure 1. Schematic diagram of the dead-end MF experimental set-up

The feed suspensions/solutions were introduced into the filtration tank. The experiments were performed under constant TMP by applying compressed nitrogen gas. The permeate weight was measured during the filtration process with an electronic balance (Ohaus Corp Pine Brook, NJ with a precision of 0.0001g). The weights were converted to volumes using density correlations. The temperature of the permeate was measured to determine its viscosity and density.

RESULTS AND DISCUSSION

Impact of operating condition on the instantaneous specific cake resistance

Impact of trans-membrane pressure

The average specific cake resistance was respectively calculated by using Eq. (4) and Eq. (5) at different pressures (Figure 2) and their relative error was 4.48% for AS suspension, 4.42% for SA solution, 11.2% for HA solution and 4.29% for BSA solution, respectively. The specific cake resistances formed by the four different feeds increased with the increase in the transmembrane pressure. This is because the porosity of the cake layer decreased with the increase of the transmembrane pressure [38]. Meanwhile, the initial trans-membrane pressure will force BSA, HA or SA to quickly deposit or adsorb the membrane surface [39,40] and force

The experimental data were recorded after each 5 seconds. The MAF-5001 model Malvern laser particle diameter distribution instrument (Britain) was used to get the particle distribution of the feed suspensions, and the modified bubble-point method was used to obtain the pore size distribution of the membrane.

bigger particles to reach the membrane surface and block more membrane pores [41,42].

In addition, SA played a leading role in the variation of the specific cake resistance of the four different feeds while BSA, HA and AS substances played a supporting role (SA>HA>BSA>AS). This can be explained by the fact that SA contains plenty of hydroxyl groups and carboxyl groups. Meanwhile, stronger intermolecular interaction results in the aggregation of SA molecules on the membrane surface to form a dense cake layer [43] while AS was bigger than the pore size of the membrane, the fouling mechanism was mainly cake formation [44] and it will form a loose cake layer.

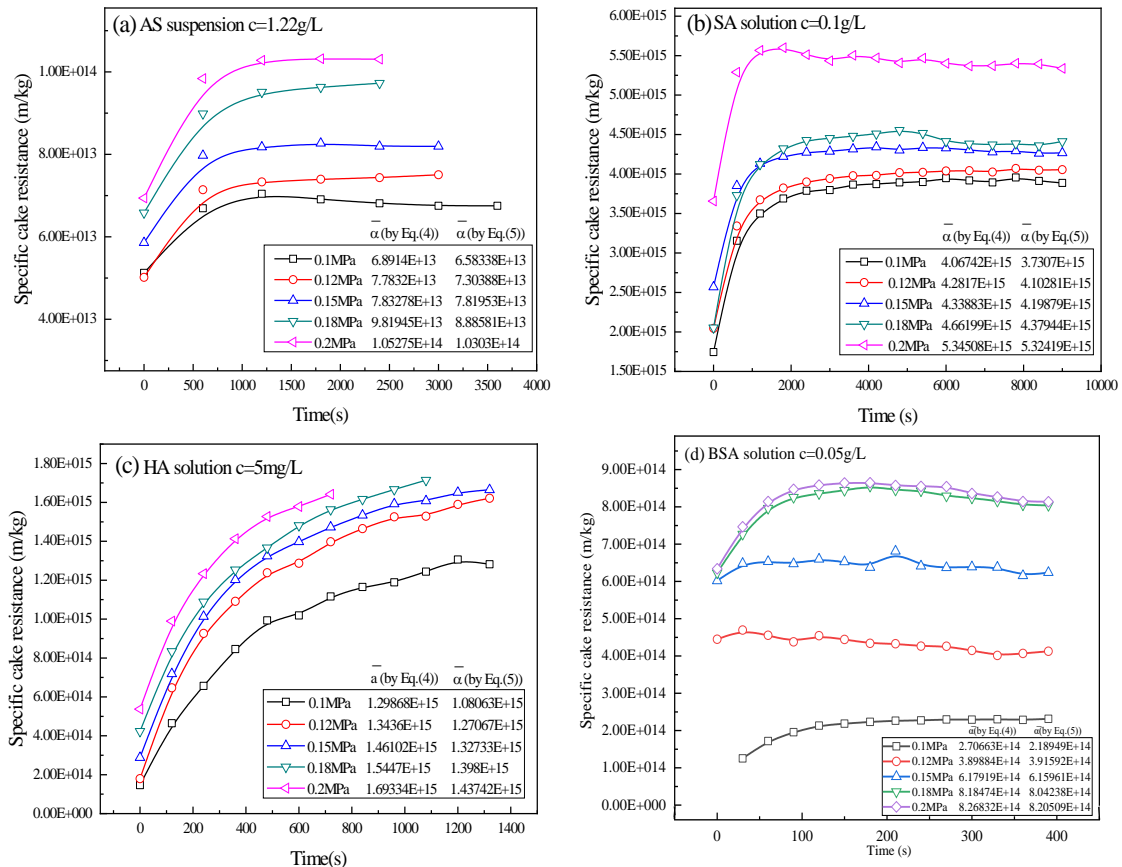


Figure 2. Comparison of specific cake resistance of AS, SA, HA, BSA at varying pressures

Impact of concentration

Different concentrations (Figure 3) and their average relative error between the specific cake resistance and average specific cake resistance was 3.13% for AS suspension, 1.94% for SA solution, 4.47% for HA solution and 6.66% for BSA solution, respectively.

Specific cake resistance increases with the increase in concentration (Figure 3). The reason is that with the increase of the mass concentration of the feed, small particles may enter the filter cake, and the obvious phenomenon of cake stratification and drilling will reduce the porosity.

The specific cake resistance basically showed an upward trend with the increase of the feed concentration [38]. SA played a leading role in the variation of the specific cake resistance, while BSA, HA and AS substances played a supporting role (SA>HA>BSA>AS). This was because higher concentration proposed a higher mass transfer coefficient [45] and a thicker cake would appear earlier on the membrane surface. Meanwhile, more small solute particles preferentially entered into cake [46], which expedited the speed of the decreasing of cake porosity.

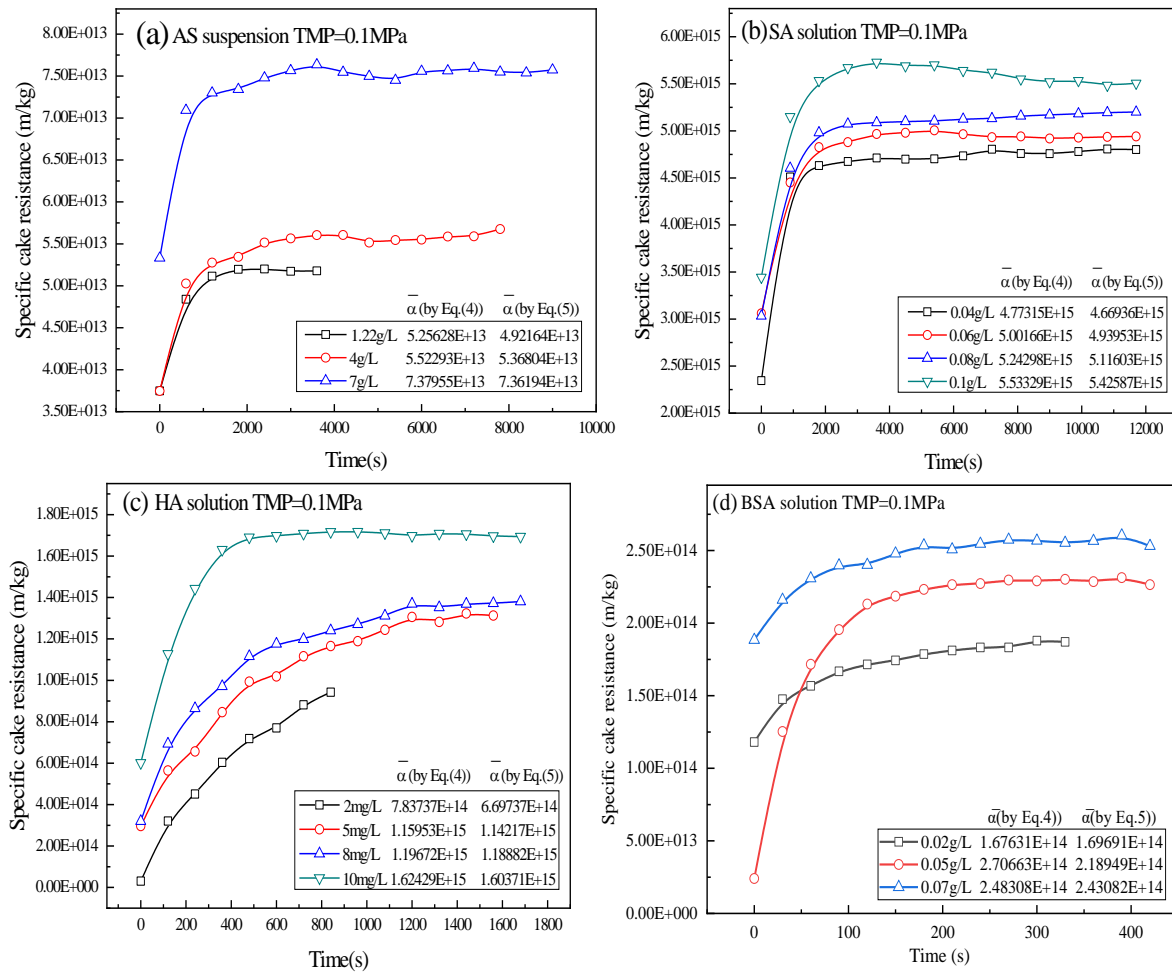


Figure 3. Comparison of specific cake resistance of AS, SA, HA, BSA at different concentrations

Impact of stirred speed

Different stirred speeds (Figure 4) and their average relative error was 10.05% for AS suspension, 39.55% for SA solution, 14.63% for HA solution, and 2.21% for BSA solution, respectively.

Specific cake resistance increases with an increase in the stirred speed (Figure 4). This is because rate upsurge increases the drag force and shear force [47], which in turn increases the reverse transmission rate of the solute particles; most of the solute is returned to bulk solution, the thickness of the inner layer of the laminar

flow is reduced, and the solute particles are deposited on the surface of the membrane, especially large particles are not easy to deposit on the membrane surface, while small particles are easy to deposit, and the final deposited layer is denser. Therefore, specific cake resistance increases with an increase in the stirred speed [38]. SA played a leading role in the variation of specific cake resistance because SA as polysaccharide was the main contributor to the membrane fouling for EPS [48], while BSA, HA, and AS substances played a supporting role (SA>HA>BSA>AS).

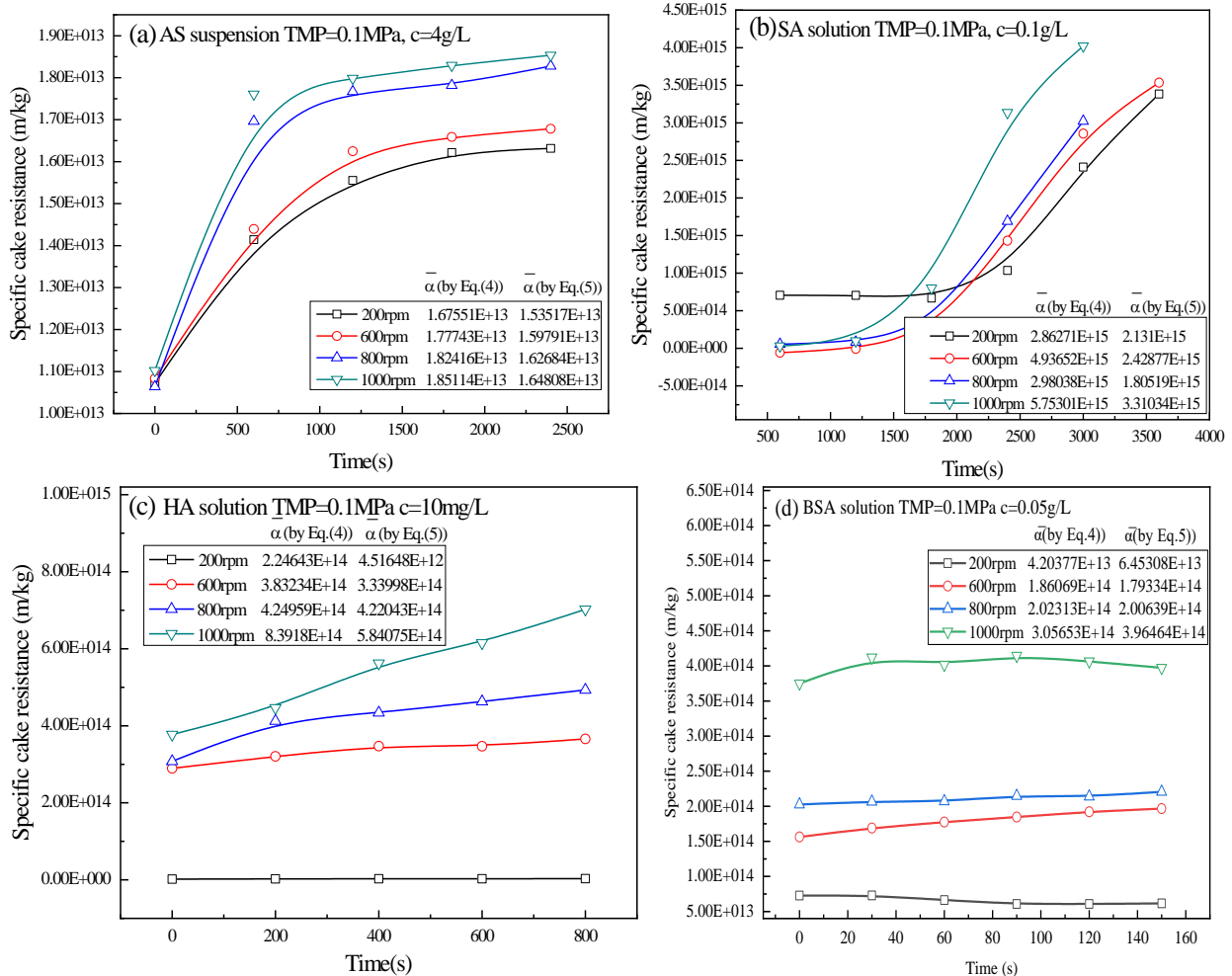


Figure 4. Comparison of specific cake resistance AS, SA, HA, and BSA at different stirred speeds

Impact of temperature

Different temperatures (Figure 5) and their average relative error was 36.5% for AS suspension, 19.1% for SA solution, 37.09% for HA solution, and 39.97% for BSA solution, respectively. Specific cake resistance decreases with an increase in the feed temperature (Figure 5). The reason is that viscosity decreases with temperature increase, while both flow rate and the drag force increase, and the bridging phenomenon is obvious. As a result, mass transfer coefficient increases, so the specific cake resistance decreases with the increase in temperature [38]. BSA played a leading role in the variation of specific cake resistance while SA, HA and AS substances played a supporting role (BSA>HA>SA>AS).

The impact of temperature on BSA is highly variable and is dependent on the microbial community and the experimental conditions. Theoretically, the increase in temperature accelerates the metabolic activity of microbes, including the secretion of EPS [49]. Higher temperatures could bring about changes in hydrodynamic conditions and sludge properties. A lower viscosity at higher temperatures could enhance shear forces and reduce the formation rate of cake layers on the membrane surfaces. In addition, the change in microbial community at different operating temperatures could also be partially responsible for the change in cake formation rate [50]. Therefore, a higher specific cake resistance was observed at lower temperature.

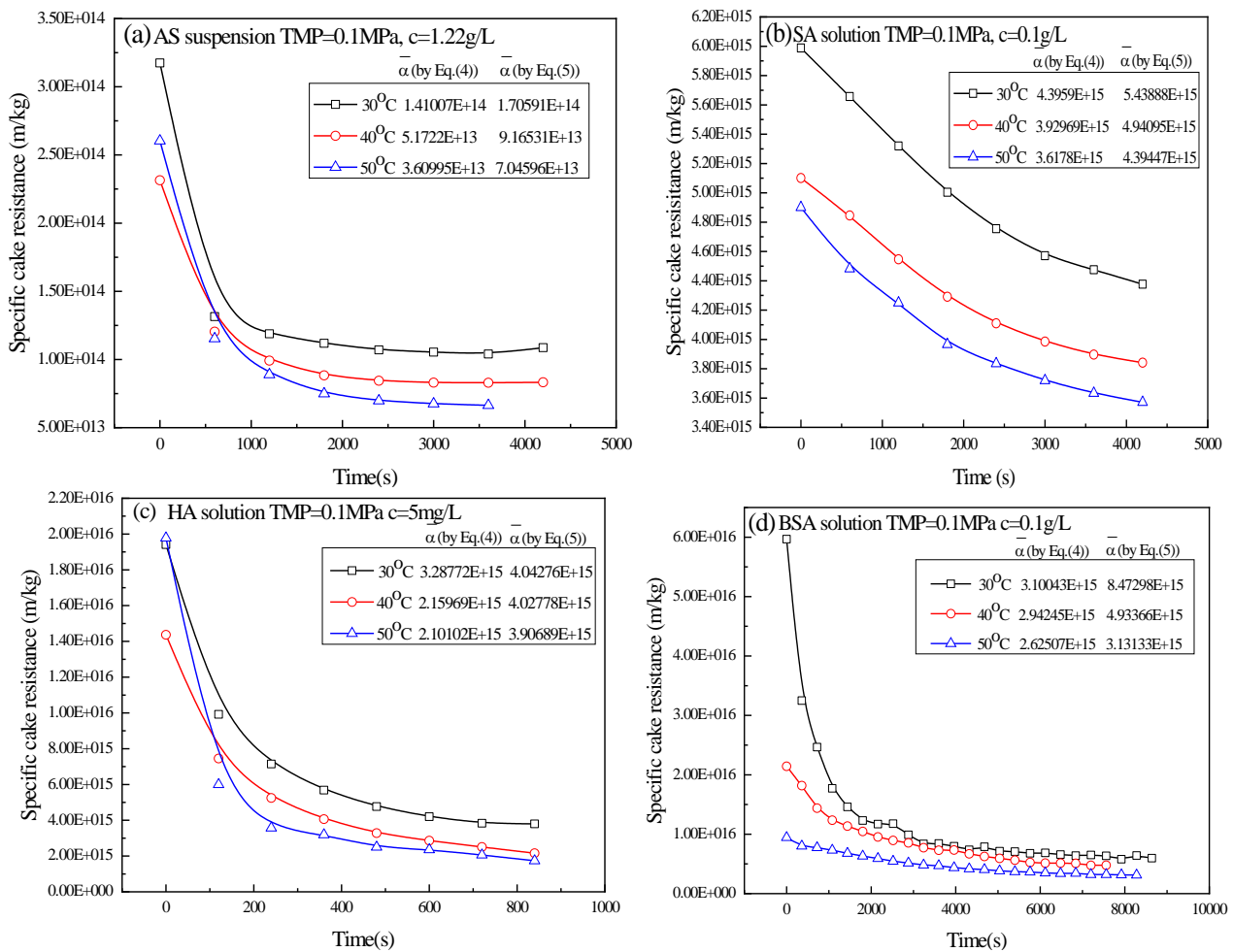


Figure 5. Comparison of specific cake resistance of AS, SA, HA, BSA at varying temperatures

Verification of calculated dates using proposed equations
Different pressure

In terms of the accuracy of the proposed model, the predicted values and the experimental data were very close at different pressures (Figure 6). Instantaneous specific cake resistance (α) markedly depends on permeate flux J (Eq.6) and on the composition of the feed solutions. Increasing α induces a decrease of permeate flux and an increase of cake resistance. Higher permeate flux was observed for higher specific cake resistance. Thus, the fouling layer formed at higher pressure would be denser, which explains the higher permeate flux observed.

The corresponding R^2/σ respectively was 0.9992/3.46%, 0.9999/4.15%, 0.9999/4.76%, 0.9991/6.35% and 0.9999/5.70% (at pressure range of 0.1MPa to 0.2MPa for AS solution), 0.9992/1.39%, 0.9999/2.00%, 0.9999/2.43%,

0.9991/3.13% and 0.9999/2.50% (at pressure range of 0.1MPa to 0.2MPa for SA solution), 0.9988/0.39%, 0.9999/0.54%, 0.9995/0.69%, 0.9996/0.85% and 0.9992/0.86% (at pressure range of 0.1MPa to 0.2MPa for HA solution), 0.9974/0.39%, 0.8237/0.49%, 0.9897/0.88%, 0.9965/2.35% and 0.9973/2.50% (at pressure range of 0.1MPa to 0.2MPa for /BSA solution). The predictions of the proposed models were in good agreement with the experimental data. Experimental results showed that the relative deviation (σ) increases with an increase in the feed pressures. This can be explained as follows: although rising TMP can increase the permeate flux, it could also facilitate concentration polarization and deposition of particles, which accelerates with the growing rate of cake layer and results in the cake compactness [51]. Following are examples of deviations between experimental and calculated values using Eq.(8).

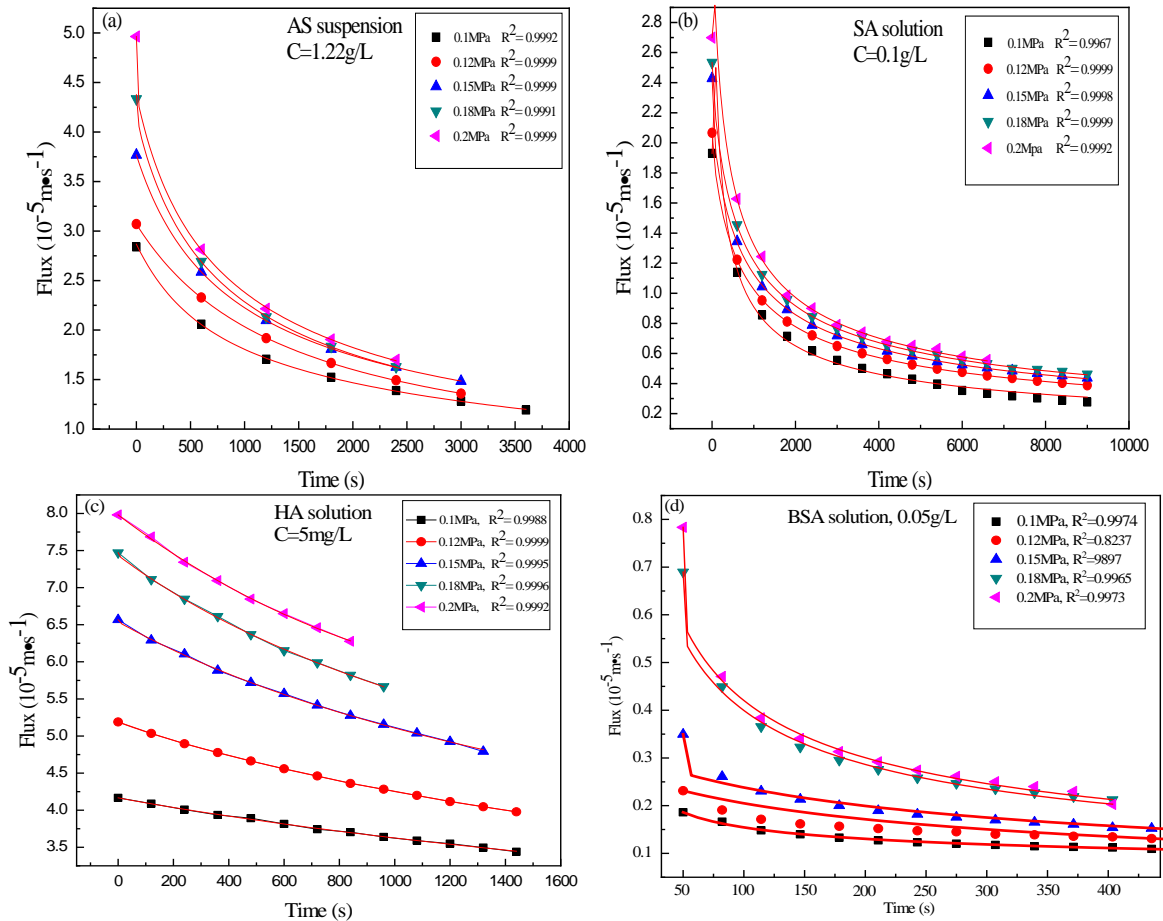


Figure 6. Comparisons of model predictions and experimental data at different pressures

Different concentration

In terms of the accuracy of the proposed model, the predicted values and the experimental data were very close at different concentrations (Figure 7). The corresponding R^2 / σ respectively was 0.9992/3.46%, 0.9998/2.72% and 0.9996/1.68% (at concentration of 1.22, 4 and 7g/L for AS suspension), 0.9221/2.55%, 0.9994/1.83%, 0.9989/1.51% and 0.9994/1.39% (at concentration of 0.04, 0.06, 0.08 and 0.1g/L for SA solution), 0.9936/0.20%, 0.9926/0.39%, 0.9998/0.49% and 0.9861/0.85% (at concentration of 2, 5, 8 and 10mg/L for HA), 0.9976/2.53%, 0.9973/2.25% and 0.9989/1.48% (at concentration of 0.02, 0.05 and 0.07g/L for BSA solution). The predictions

of the proposed models were in good agreement with the experimental data. The experimental results showed that the relative deviation (σ) decreases with the increase of the feed concentrations. The flux of AS suspension and HA solution decreased rapidly compared to that of SA and BSA solution at the same concentration owing to different particle sizes of SA and BSA. This can be explained by the fact that the increase in feed concentration will enhance concentration polarization as well as adsorption of substance, which results in the enhancement of the resistance, and in the cake thickening also speeds up. Therefore, the cake layer became more densely packed, and thus the corresponding membrane flux will be decreased [51].

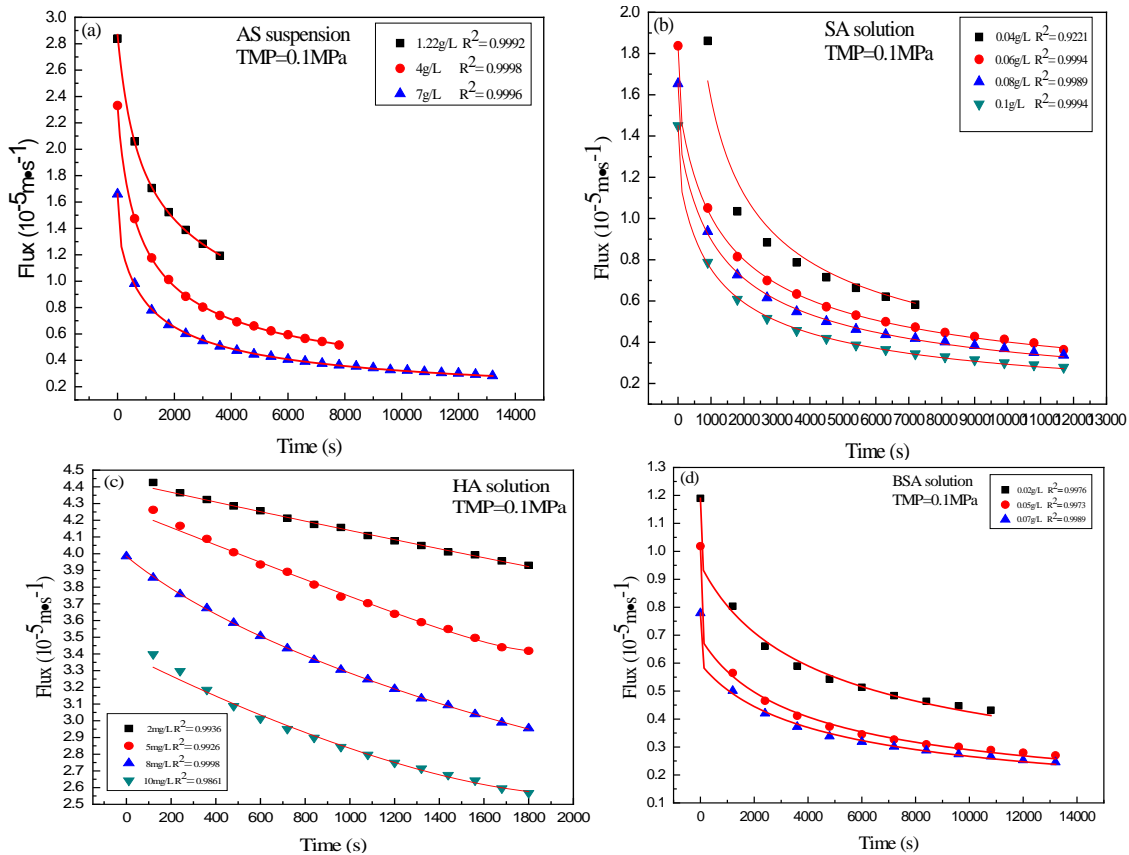


Figure 7. Comparisons of model predictions and experiment data at different concentrations

Different stirred speed

The predicted values and the experimental data were very close at different stirred speeds (Figure 8). The corresponding R^2/σ respectively was 0.9999/2.35%, 0.9999/5.84%, 0.9981/5.31% and 0.9956/5.11% (at stirred speed of 200, 600, 800 and 1000 rpm for AS suspension), 0.5746/12.54%, 0.7668/23.52%, 0.7816/23.07% and 0.8256/25.30% (at stirred speed of 200, 600, 800 and 1000 rpm for SA solution), 0.9841/0.36%, 0.9604/0.53%,

0.9578/0.44% and 0.9455/0.49% (at stirred speed of 200, 600, 800 and 1000 rpm for HA solution), 0.9045/3.69%, 0.9451/1.39% 0.9135/1.01% and 1.00/0.72% (at stirred speed of 200, 600, 800 and 1000 rpm for BSA solution). The experimental results showed that the relative deviations (σ) increases with the increase of the stirred speed. A higher stirred speed results in faster cake growth while the filtration process is longer at a low stirred speed due to low cake resistance [52].

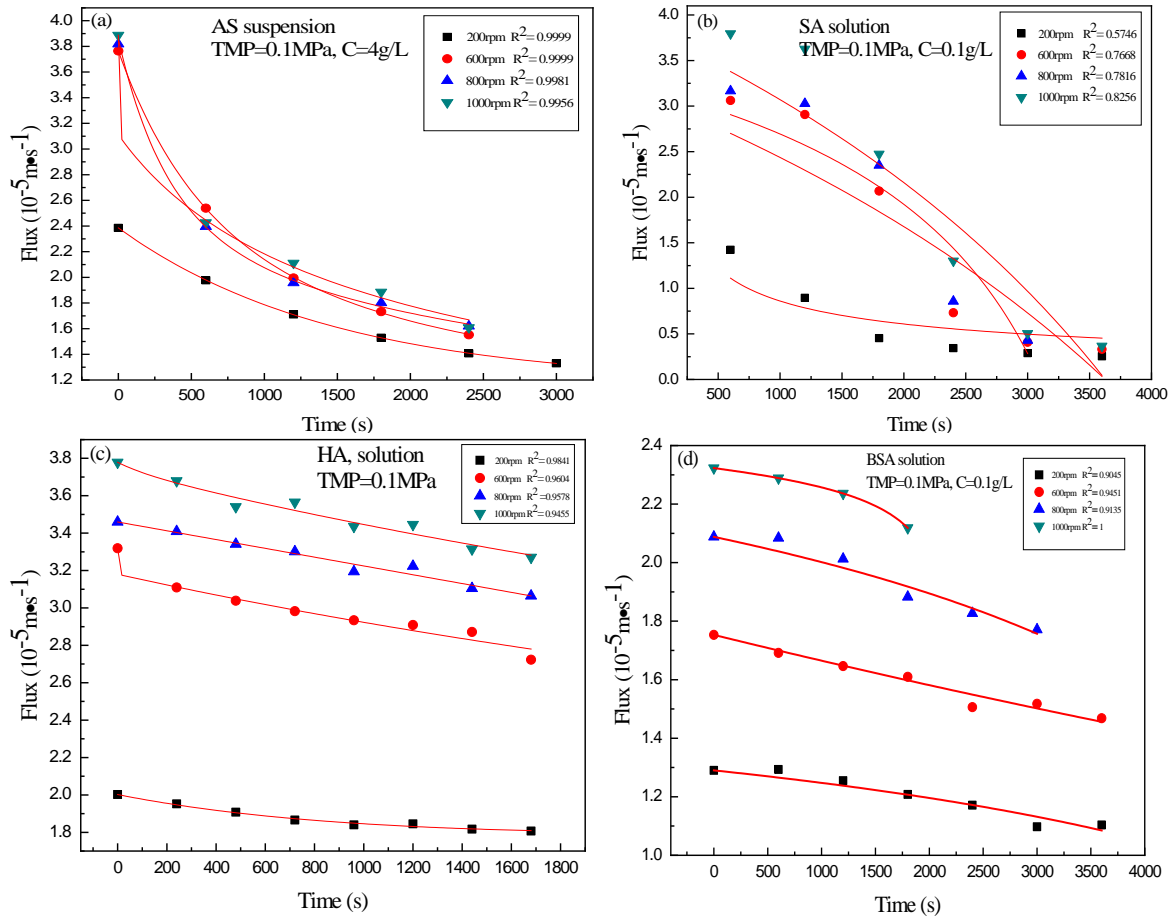


Figure 8. Comparisons of model predictions and experiment data at different stirred speeds

Different temperatures

The predicted values and the experimental data were very close at different temperatures (Figure 9). The corresponding R^2/σ respectively was 0.9246/1.09%, 0.9038/1.77% and 0.9754/1.65% (at temperature of 30, 40 and 50°C for AS suspension), 0.9995/2.54%, 0.9999/2.44% and 0.9999/2.76% (at temperature of 30, 40 and 50°C for SA solution), 0.9893/0.15%, 0.9993/20.22% and 0.9997/0.23% (at temperature of 30, 40 and 50°C for HA solution),

0.9988/0.34% 0.9412/0.74% and 0.9847/0.62% (at temperature of 30, 40 and 50°C for BSA solution). The experimental results showed that the relative deviations (σ) were first increased but then again decreased because of the fact that the permeate flux is inversely proportional to fluid viscosity. As the temperature was raised, the viscosity of the permeate decreased, and mass-transfer coefficient increased, and these two effects together lead to a higher permeate flux at a higher temperature [51].

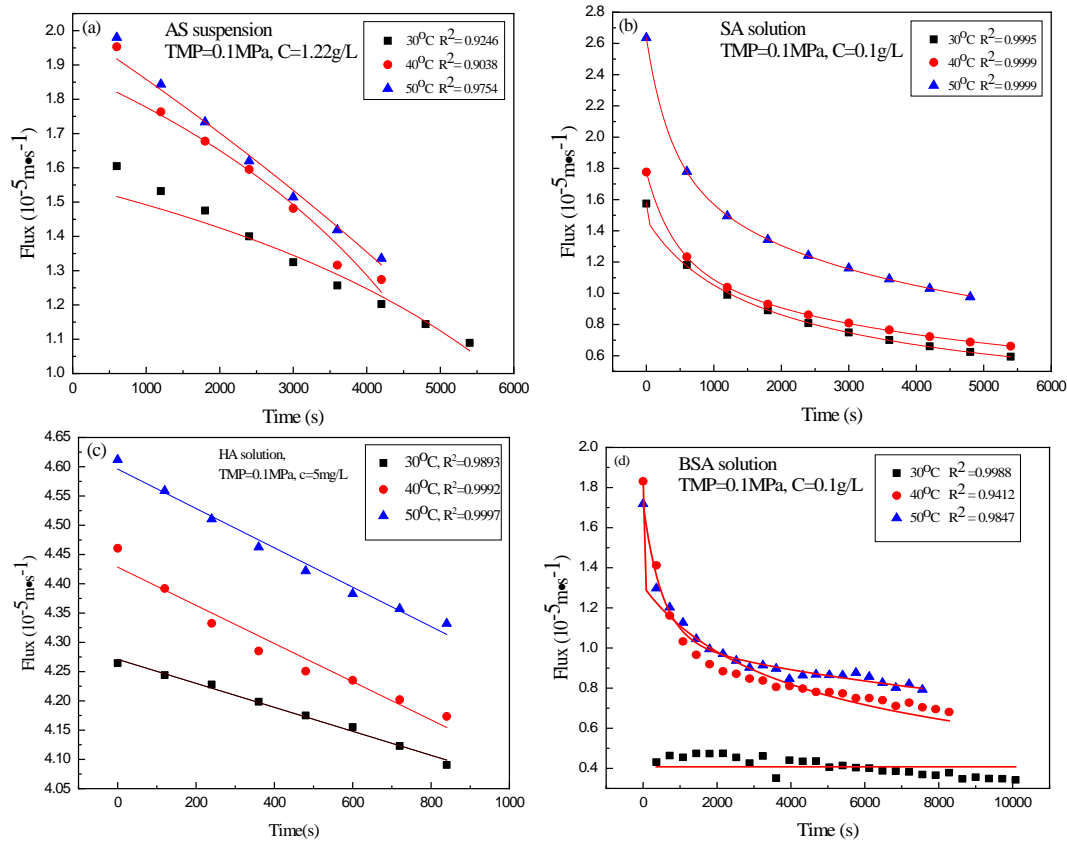


Figure 9. Comparisons of model predictions and experiment data at different temperatures

The resistance analysis

The fouling mechanism

The fouling mechanism for AS suspension and SA solution is almost cake filtration due to the fact that a straight line was observed for AS suspension and SA solution (Fig.10(a)) and the corresponding cake resistance possesses a decisive percentage in the total resistance (AS suspension (R_c 80%, R₀ 15% and R_b 5%) and SA solution (R_c 70%, R₀

10%, R_b 20%) (Figure 10 (b)) while the fouling mechanism for HA and BSA solutions was a combined mechanism because the straight line deviates from the experimental data (Figure 10(a)) and there is a certain component of the pore blocking resistance in the total resistance (HA solution (R_c 30%, R₀ 65%, R_b 5%))and BSA solution (R_c 60%, R₀ 15%, R_b 25%)) (Fig.10(b)).

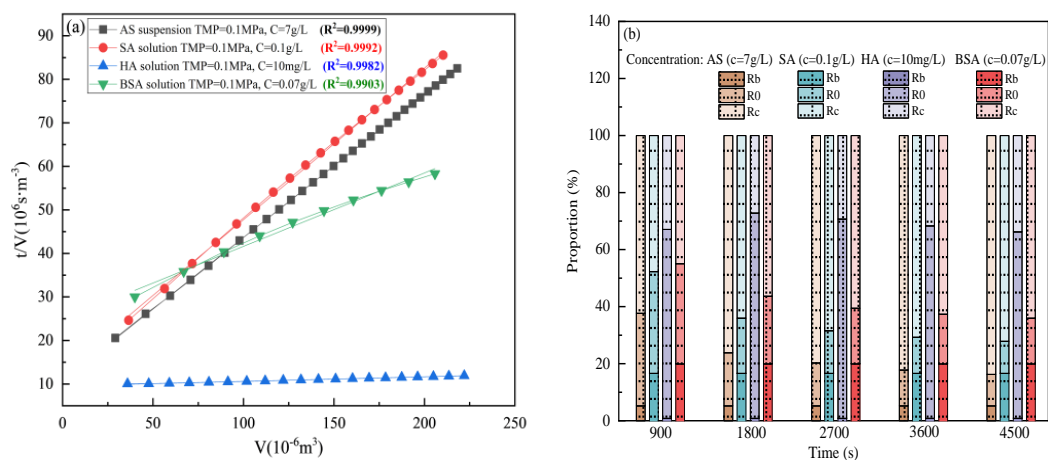


Figure 10. Ratio of filtration time and filtration volume as a function of total filtrate volume. (a) AS suspension at TMP of 0.1MPa and concentration of 7g/L, (b) SA solution at TMP of 0.1MPa and concentration of 0.1g/L, (c) HA solution at TMP of 0.1MPa and concentration of 10mg/L, (d) BSA solution at TMP of 0.1MPa and concentration of C=0.07g/L

The different resistance analysis

The resistances (R_b , R_0 and R_c) were calculated by using the method described in reference [17] and the corresponding results were shown in Figure 11-14. The percentage of the cake resistance in the total resistance was 80%, 70%, 20%, and 60% for AS suspension, SA solution, HA solution, and BSA solution respectively. This indicated that the cake resistance for AS and SA solutions were the

largest, whereas that for HA and BSA solutions was the smallest. Meanwhile, the percentage of complete blocking resistance in the total resistance for AS suspension and SA solution was the largest, whereas it was the smallest for HA and BSA solution. This is because the fouling mechanism for AS suspension and SA solution was cake filtration, while that for HA and BSA, it was a combined mechanism.

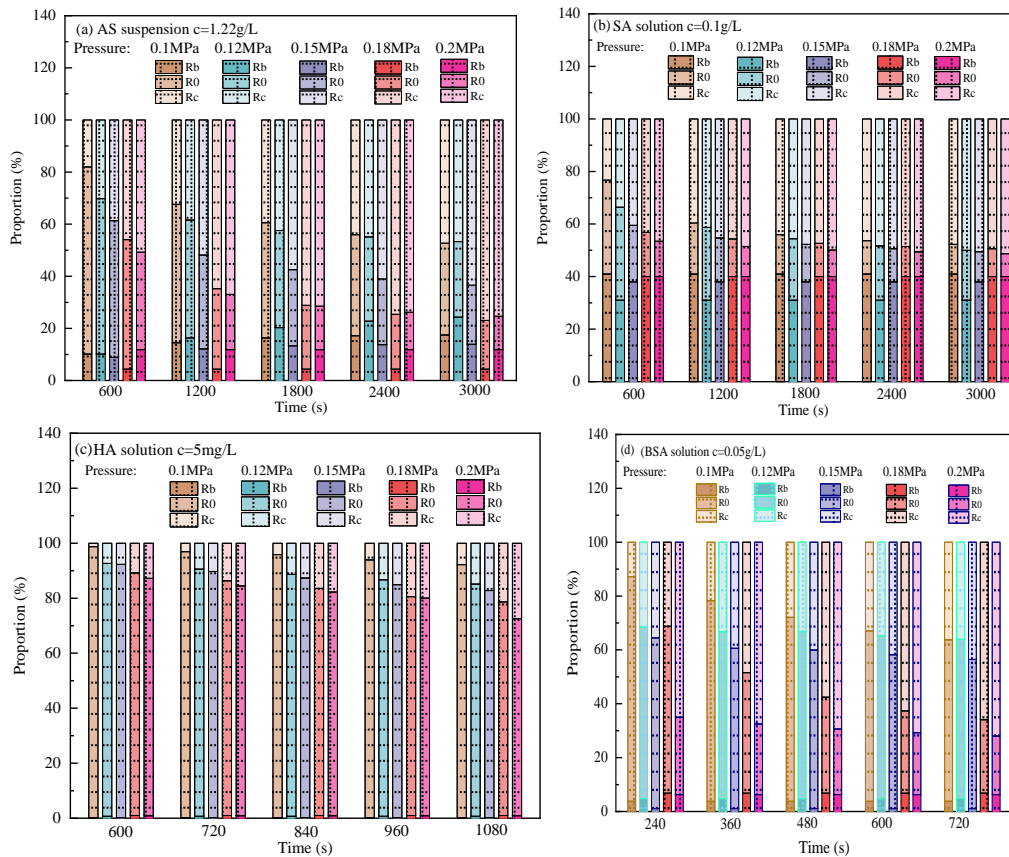


Figure 11. Virgin membrane resistance (R_0), cake resistance (R_c), and complete blocking resistance (R_b) as a function of time by using PES 0.1 μ m membrane at different pressures

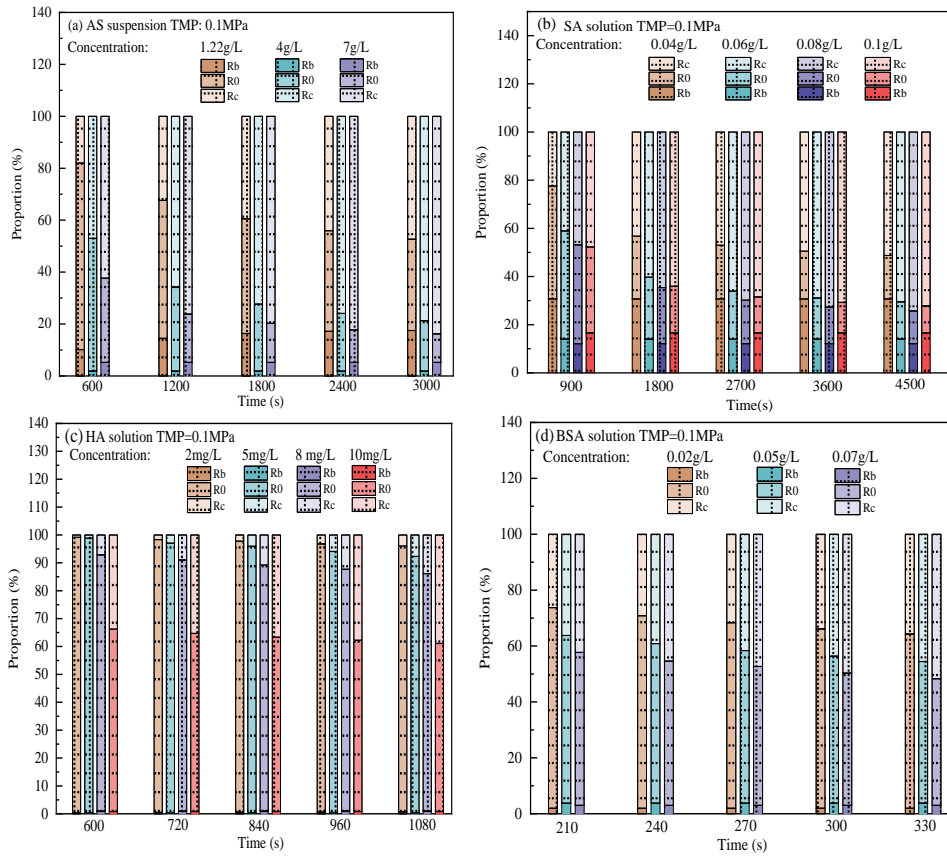


Figure 12. Virgin membrane resistance (R_0), cake resistance (R_c), and complete blocking resistance (R_b) as a function of time by using PES 0.1 μ m membrane at different concentrations

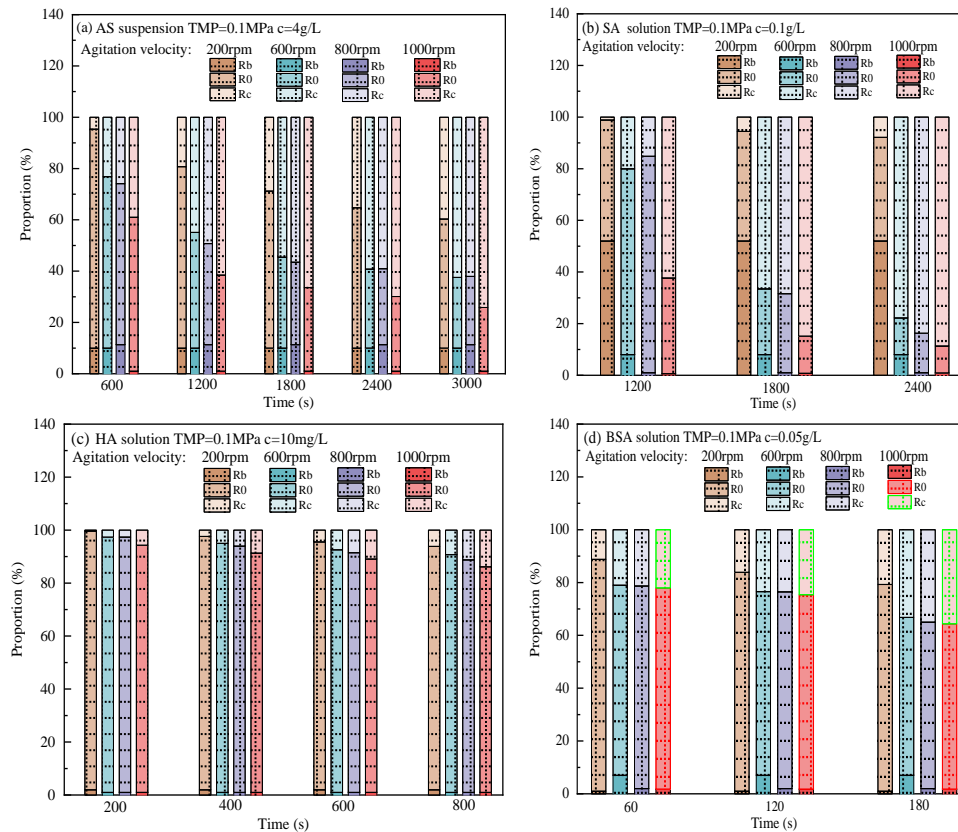


Figure 13. Virgin membrane resistance (R_0), cake resistance (R_c), and complete blocking resistance (R_b) as a function of time by using PES 0.1 μ m membrane at different stirred speeds

The cake resistance and its proportion in the total resistance decreased with the increase of temperature (Figure 14). The fouling resistance is expected to reduce because viscosity decreases and permeability increases at higher temperatures. Furthermore, the shear stress on the membrane surface is expected to increase with an increase in temperature, due to the viscosity reduced at higher temperatures [50]. As temperature increases, the higher permeate flux will be obtained at higher temperature due to lower viscosity and higher mass-transfer coefficient [53,54]. Moreover, these facts increase the drag force for solute particles and the bridge phenomena becomes insignificant. As a result, solute particles do not

deposit easily on the membrane surface and the formed cake would be lost [7].

In addition, average specific cake resistance calculated by using Eq.(4) and that calculated by Eq.(5) is very close to each other for AS suspension and SA solution because the Eq.(4) was obtained based on cake filtration mechanism, while this result was far from each other for HA solution and BSA solution, because their fouling mechanism is a combined mechanism instead of cake filtration (Figure 2- Figure 5). In contrast, the predictive values of the proposed equation of the specific cake resistance and the experimental data are in good agreement at operating conditions for AS suspension and four different solutions (SA, HA, BSA) (Figure 2).

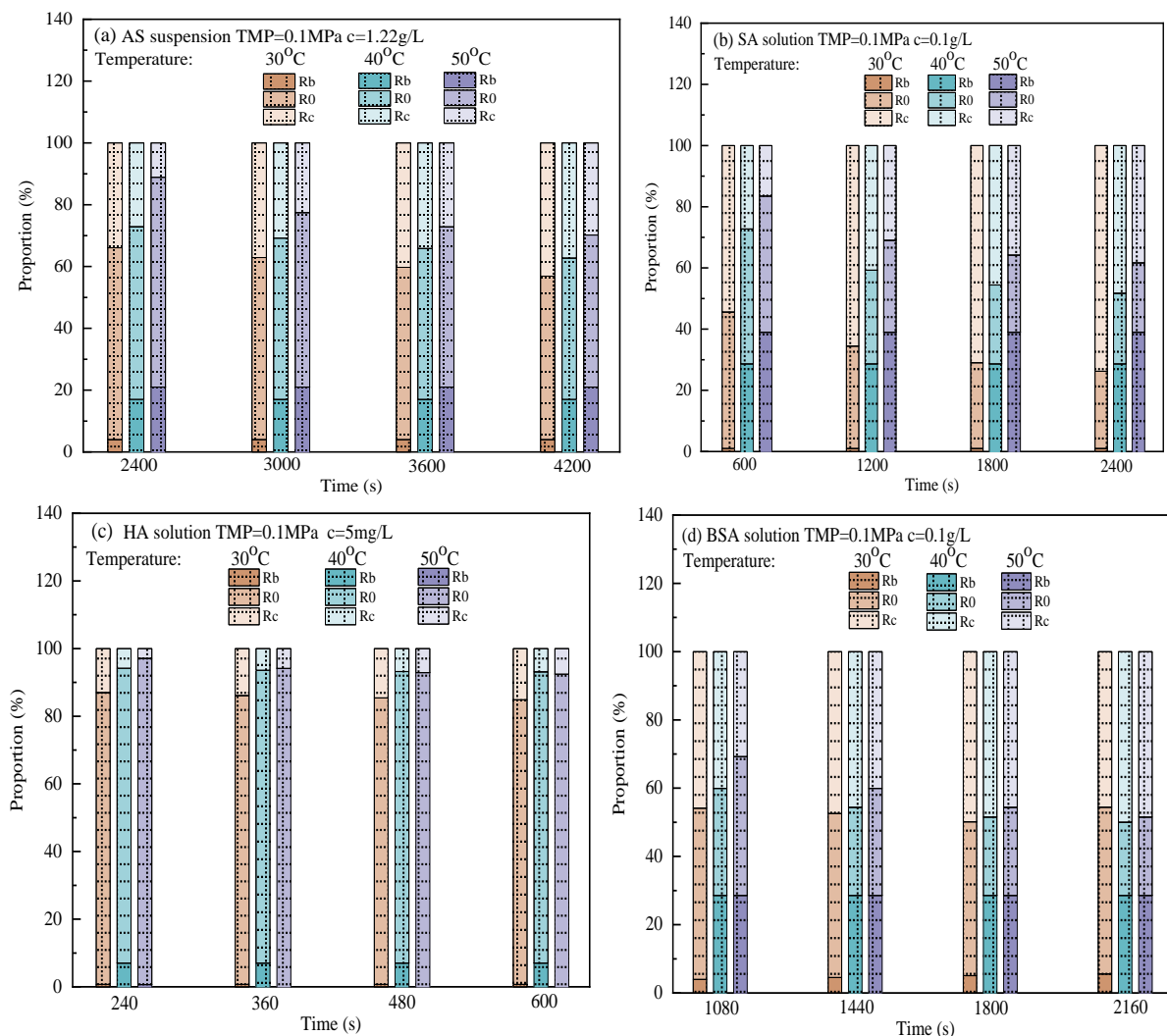


Figure 14. Virgin membrane resistance (R_0), cake resistance (R_c), and complete blocking resistance (R_b) as a function of time at 0.1MPa, at 1.22 g/L for AS, 0.1g/L for SA, 5mg/L for HA, 0.1 g/L for BSA, and temperature in the range of 30°C, 40°C to 50°C by using 0.1 μ m PES membrane

CONCLUSIONS

The results showed that the proposed equation can be used to accurately calculate instantaneous specific cake resistance (α). The following conclusions were drawn:

- Specific cake resistances formed by four different feeds increased with the increase in the transmembrane pressure. SA played a leading role in the variation of the specific cake resistance of the four different feeds, while BSA, HA and AS substances played a supporting role SA>HA >BSA >AS.
- Specific cake resistance increases with an increase of concentration. Specific cake resistance basically showed an upward trend with the increase of the feed concentration.
- Therefore, specific cake resistance increases with the increase of the stirred speed.
- Specific cake resistance decreases with the increase of the feed temperature. Therefore, a higher specific cake resistance was observed at a lower temperature.

- The predictions of the proposed equation were in good agreement with the experimental data ($R^2>0.99$) and the relative deviations (σ) increased with the increase in the feed pressures and stirred speed, while it decreases with the increase of the feed concentration and temperature.
- SA possess higher specific cake resistance compared to BSA solution, HA solution and AS suspension. The fouling mechanism of HA and AS is cake formation while that of BSA and SA is cake formation and pore blocking. Moreover, cake resistance (R_c) and complete blocking resistance (R_b) increased with the increase pressures, concentration and stirred speed. While the cake resistance (R_c) and complete blocking resistance (R_b) decreased with the increase in temperature. The complete blocking resistance (R_b) for SA is larger than that for BSA, HA and AS, whereas the specific cake resistance follows the following sequence:SA>HA>BSA>AS.

REFERENCES

1. M. Elimelech, W. A. Phillip, The future of seawater desalination: Energy, technology, and the environment. *Science*, 333 (2011), pp.712-717
<https://doi.org/10.1126/science.1200488>
2. M. A. Shannon, P. W. Bohn, M. Elimelech, J. G. Georgiadis, B. J. Marin, A. M. Mayes, Science and technology for water purification in the coming decades. *Nature*, 452 (2008), pp.301-310.
<https://doi.org/10.1038/nature06599>
3. Alireza Zirehpour, Ahmad Rahimpour, *Membranes for Wastewater Treatment*, 2, (2016), pp. 159-208.
<https://doi.org/10.1002/9781118831823.ch4>
4. P. Blanpain, J. Hermia and M. Lenoel, Mechanisms governing permeation flux and protein rejection in the MF of beer with a Cyclopore membrane, *J. Membr.Sc.*, 84 (1993), pp. 37-51.
[https://doi.org/10.1016/0376-7388\(93\)85049-3](https://doi.org/10.1016/0376-7388(93)85049-3)
5. A. Filippov, V. M. Starov, D. R. Lloyd, S. Chakravarti and S. Glaser, Sieve mechanism of microfiltration, *J. Membr.Sc.*, 89 (1994), pp.199-213.
[https://doi.org/10.1016/0376-7388\(94\)80102-9](https://doi.org/10.1016/0376-7388(94)80102-9)
6. G. Belfort, R. H. Davis and A. L. Zydney, The behavior of suspensions and macromolecular solutions in cross-flow microfiltration, *J.Membr.Sci.*, 96 (1994), pp. 1-58.
[https://doi.org/10.1016/0376-7388\(94\)00119-7](https://doi.org/10.1016/0376-7388(94)00119-7)
7. Zhan Wang, Ximing Zhang, Xu Wang & Yawen Lyu, Accumulated impact of operating conditions on the specific cake resistance in dead-end microfiltration mode, *Desalination and Water Treatment* , 57:5, pp.1967-1976.
<https://doi.org/10.1080/19443994.2014.983178>
8. O. T. Iorhemen, R. A. Hamza, J. H. Tay, Membrane fouling control in membrane bioreactors (MBRs) using granular materials, *Bioresour. Technol.* 240 (2017) pp. 9-24.
<https://doi.org/10.1016/j.biortech.2017.03.005>
9. J. Wu, C. He, X. Jiang, M. Zhang, Modeling of the submerged membrane bioreactor fouling

- by the combined pore constriction, pore blockage and cake formation mechanisms, *Desalination* 279 (2011) pp. 127-134.
<https://doi.org/10.1016/j.desal.2011.05.069>
10. C. Caudan, A. Filali, M. Sperandio, E. Girbal-Neuhausser, Multiple EPS interactions involved in the cohesion and structure of aerobic granules, *Chemosphere* 117 (2014) pp. 262-270.
<https://doi.org/10.1016/j.chemosphere.2014.07.020>
 11. H. Lin, M. Zhang, F. Wang, F. Meng, B. Q. Liao, H. Hong, J. Chen, W. Gao, A critical review of extracellular polymeric substances (EPSs) in membrane bioreactors: characteristics, roles in membrane fouling and control strategies, *J. Membr. Sci.* 460 (2014) pp. 110-125.
<https://doi.org/10.1016/j.memsci.2014.02.034>
 12. W. Yao, Z. Wang, P. Song, The cake layer formation in the early stage of filtration in MBR: mechanism and model, *J. Membr. Sci.* 559 (2018) pp. 75-86.
<https://doi.org/10.1016/j.memsci.2018.04.042>
 13. D. P. Saroj, G. Guglielmi, D. Chiarani, G. Andreottola, Modeling and simulation of membrane bioreactors by incorporating simultaneous storage and growth concept: an especial attention to fouling while modeling the biological process, *Desalination* 221 (2008) pp. 475-482.
<https://doi.org/10.1016/j.desal.2007.01.108>
 14. S. T. Kelly, A. L. Zydney, Mechanisms for bsa fouling during microfiltration, *J. Membr. Sci.* 107 (1995) pp. 115-127.
[https://doi.org/10.1016/0376-7388\(95\)00108-Q](https://doi.org/10.1016/0376-7388(95)00108-Q)
 15. K. Katsoufidou, S. Yiantsios, A. Karabelas, A study of ultrafiltration membrane fouling by humic acids and flux recovery by backwashing: experiments and modeling, *J. Membr. Sci.* 266 (2005) pp. 40-50.
<https://doi.org/10.1016/j.memsci.2005.05.009>
 16. C. Duclos-Orsello, W. Li, C. C. Ho, A three mechanism model to describe fouling of microfiltration membranes, *J. Membr. Sci.* 280 (2006) pp. 856-866.
<https://doi.org/10.1016/j.memsci.2006.03.005>
 17. L. Hou, Z. Wang, P. Song, A precise combined complete blocking and cake filtration model for describing the flux variation in membrane filtration process with BSA solution, *J. Membr. Sci.* 542 (2017) pp. 186-194.
<https://doi.org/10.1016/j.memsci.2017.08.013>
 18. J. Wu, C. He, X. Jiang, M. Zhang, Modeling of the submerged membrane bioreactor fouling by the combined pore constriction, pore blockage and cake formation mechanisms, *Desalination* 279 (2011) pp. 127-134.
<https://doi.org/10.1016/j.desal.2011.05.069>
 19. S. T. Kelly, A. L. Zydney, Mechanisms for bsa fouling during microfiltration, *J. Membr. Sci.* 107 (1995) pp. 115-127.
[https://doi.org/10.1016/0376-7388\(95\)00108-Q](https://doi.org/10.1016/0376-7388(95)00108-Q)
 20. C. C. Ho, A. L. Zydney, A combined pore blockage and cake filtration model for protein fouling during microfiltration, *J. Colloid Interface Sci.* 232 (2000) pp. 389-399.
<https://doi.org/10.1006/jcis.2000.7231>
 21. G. Bolton, D. Lacasse, R. Kuriyel, Combined models of membrane fouling: development and application to microfiltration and ultrafiltration of biological fluids, *J. Membr. Sci.* 277 (2006) pp. 75-84.
<https://doi.org/10.1016/j.memsci.2004.12.053>
 22. C. Duclos-Orsello, W. Li, C. C. Ho, A three mechanism model to describe fouling of microfiltration membranes, *J. Membr. Sci.* 280 (2006) pp. 856-866.
<https://doi.org/10.1016/j.memsci.2006.03.005>
 23. W. Yuan, A. Kocic, A. L. Zydney, Analysis of humic acid fouling during microfiltration using a pore blockage-cake filtration model, *J. Membr. Sci.* 198 (2002) pp. 51-62.
[https://doi.org/10.1016/S0376-7388\(01\)00622-6](https://doi.org/10.1016/S0376-7388(01)00622-6)
 24. K. Katsoufidou, S. Yiantsios, A. Karabelas, A study of ultrafiltration membrane fouling by humic acids and flux recovery by backwashing: experiments and modeling, *J. Membr. Sci.* 266 (2005) pp. 40-50
<https://doi.org/10.1016/j.memsci.2005.05.009>
 25. Y. Ye, V. Chen, A.G. Fane, Modeling long-term subcritical filtration of model EPS solutions, *Desalination* 191 (2006) 318-327
<https://doi.org/10.1016/j.desal.2005.04.128>
 26. J. Wu, C. He, X. Jiang, M. Zhang, Modeling of the submerged membrane bioreactor fouling by the combined pore constriction, pore blockage and cake formation mechanisms, *Desalination* 279 (2011) 127-134
<https://doi.org/10.1016/j.desal.2011.05.069>
 27. E. Iritani, Y. Mukai, Y. Tanaka, T. Murase, Flux decline behavior in dead-end microfiltration of protein solutions, *J. Membr. Sci.* 103 (1995), pp.181-191
[https://doi.org/10.1016/0376-7388\(94\)00321-Q](https://doi.org/10.1016/0376-7388(94)00321-Q)
 28. J. Sripui, C. Pradistsuwana, W.L. Kerr, P. Pradipasena, Effects of particle size and its distribution on specific cake resistance during

- rice wine microfiltration, *J. Food. Eng.* 105 (2011), pp.73-78
<https://doi.org/10.1016/j.jfoodeng.2011.01.033>
29. S.A. Lee, A.G. Fane, R. Amal, The effect of floc size and structure on specific cake resistance and compressibility in dead-end microfiltration, *Sep. Sci. Technol.* 38 (2003), pp.869-887
<https://doi.org/10.1081/SS-120017631>
 30. N.M. Jenny, G. Foley, Dead-end filtration of yeast suspensions: Correlating specific resistance and flux data using artificial neural networks, *J. Membr. Sci.* 281 (2006), pp.325-333
<https://doi.org/10.1016/j.memsci.2006.03.043>
 31. M. Mota, J.A. Teixeira, Influence of cell-shape on the cake resistance in dead-end and cross-flow filtrations, *Sep. Purif. Technol.* 27 (2002), pp.137-144
[https://doi.org/10.1016/S1383-5866\(01\)00202-7](https://doi.org/10.1016/S1383-5866(01)00202-7)
 32. K. Ohmori, C.E. Glatz, Effects of pH and ionic strength on microfiltration of *C. glutamicum*, *J. Membr. Sci.* 153 (1999), pp.23-32.
[https://doi.org/10.1016/S0376-7388\(98\)00239-7](https://doi.org/10.1016/S0376-7388(98)00239-7)
 33. [Application of linear multi-regression model for specific resistance study in the dead-end microfiltration - Details - 北京工业大学机构库 \(inoteexpress.com\)](https://doi.org/10.1016/S0376-7388(98)00239-7)
 34. Dimitrios Sioutopoulos, Anastasios Karabelas, Vasileios Mappas, Membrane Fouling Due to Protein-Polysaccharide Mixtures in Dead-End Ultrafiltration; the Effect of Permeation Flux on Fouling Resistance, 19 (2019), pp. 3-4.
<https://doi.org/10.3390/membranes9020021>
 35. Sutzkover-Gutman, D. Hasson, R. Semiat, Humic substances fouling in ultrafiltration processes, *Desalination* , 261 (2010), pp. 218-231.
<https://doi.org/10.1016/j.desal.2010.05.008>
 36. C. Halle, P .M. Huck, S. Peldszus, J. Haberkamp, M. Jekel, Assessing the performance of biological filtration as pretreatment to low pressure membranes for drinking water, *Environ. Sci. Technol.*, 43 (2009), pp. 3878-3884.
<https://doi.org/10.1021/es803615g>
 37. Zhan Wang, Shanshan Zhao, Feng Liu, Liying Yang, Yin Song, Xiuyan Wang, Xuejie Xi, Influence of operating conditions on cleaning efficiency in sequencing batch reactor (SBR) activated sludge process -water rinsing introduced membrane filtration process, *Desalination* 259 (2010), pp. 235-242.
<https://doi.org/10.1016/j.desal.2010.03.048>
 38. [中空纤维微滤膜污染及阻力分析 - 百度学术 \(baidu.com\)](https://doi.org/10.1016/j.desal.2010.03.048)
 39. K. Akamatsu, Y. Kagami, S. i. Nakao, Effect of BSA and sodium alginate adsorption on decline of filtrate flux through polyethylene microfiltration membranes, *J. Membr. Sci.* (2020) p. 594.
<https://doi.org/10.1016/j.memsci.2019.117469>
 40. M. Hashino, K. Hiram, T. Ishigami, Y. Ohmukai, T. Maruyama, N. Kubota, H. Matsuyama, Effect of kinds of membrane materials on membrane fouling with BSA, *J. Membr. Sci.* 384 (2011) pp. 157-165.
<https://doi.org/10.1016/j.memsci.2011.09.015>
 41. W. Yuan, A.L. Zydney, Humic acid fouling during microfiltration, *J. Membr. Sci.* 157 (1999) pp. 1-12.
[https://doi.org/10.1016/S0376-7388\(98\)00329-9](https://doi.org/10.1016/S0376-7388(98)00329-9)
 42. Y. Hao, A. Moriya, T. Maruyama, Y. Ohmukai, H. Matsuyama, Effect of metal ions on humic acid fouling of hollow fiber ultrafiltration membrane, *J. Membr. Sci.* 376 (2011) pp. 247-253.
<https://doi.org/10.1016/j.memsci.2011.04.035>
 43. Hou. D., Lin, D.,Zhao, C., Wang, J. Fu, C. 2017 Control of protein (BSA) fouling by ultrasonic irradiation during membrane distillation process. *Separation and Purification Technology* pp. 175, 287-297.
<https://doi.org/10.1016/j.seppur.2016.11.047>
 44. F. Xiao, P. Xiao, W. J. Zhang, D. S. Wang, Identification of key factors affecting the organic fouling on low-pressure ultrafiltration membranes, *J. Membr. Sci.* 447 (2013) pp. 144-152.
<https://doi.org/10.1016/j.memsci.2013.07.040>
 45. S. Nataraj, R. Schomäcker, M. Kraume, I .M. Mishra, A. Drews, Analyses of polysaccharide fouling mechanisms during crossflow membrane filtration, *J. Membr.Sci.* 308 (2008) pp. 152-161.
<https://doi.org/10.1016/j.memsci.2007.09.060>
 46. G. Foley, P. F. MacLoughlin, D .M. Malone, Preferential deposition of smaller cells during cross-flow microfiltration of a yeast suspension, *Biotechnol. Tech.* 6 (1992) pp. 115-120.
<https://doi.org/10.1007/BF02438815>
 47. Kuo-Jen Hwang, Syuan-Jyun Lin, Filtration flux-shear stress-cake mass relationships in microalgae rotating-disk dynamic microfiltration, *J. Chemical Engineering* 244 (2014) pp. 429-437.

48. <https://doi.org/10.1016/j.cej.2014.01.076>
Amine Charfi, Fida Tibi, Jeonghwan Kim, Jin Hur and Jinwoo Cho, Organic Fouling Impact in a Direct Contact Membrane Distillation System Treating Wastewater: Experimental Observations and Modeling Approach, 2021, 11(7): p. 493.
49. <https://doi.org/10.3390/membranes11070493>
G. J. Grobber, J. Sikkema, M. R. Smith, J. A. M. D. Bont, Production of extracellular polysaccharides by *Lactobacillus delbrueckii* spp. *bulgaricus* NCFB 2772 grown in a chemically defined medium, *J. Appl. Bacteriol.* 79 (1995) pp. 103-107.
<https://doi.org/10.1111/j.1365-2672.1995.tb03130.x>
50. P. van den Brink, O. A. Satpradit, A. van Bentem, A. Zwijnenburg, H. Temmink, M. van Loosdrecht, Effect of temperature shocks on membrane fouling in membrane bioreactors, *Water Res.* 45 (2011) pp. 4491-4500.
<https://doi.org/10.1016/j.watres.2011.05.046>
51. Zhan Wang, Liying Yang, Yawen Lyu, Martculevich Nikolai Aleksandrov, Qian Zhang, Dezhong Liu, and Xining Zhang, Study of Dead-End Microfiltration Flux Variety Law, PartII: Choice of Favorable Model Parameter Separation Science and Technology, 2014, 49 (17) pp. 2657-2667.
<https://doi.org/10.1080/01496395.2014.941489>
52. Mahmood Saleem, Gernot Krammer, M. Suleman Tahir, The effect of operating conditions on resistance parameters of filter media and limestone dust cake for uniformly loaded needle felts in a pilot scale test facility at ambient conditions, 228 (2012) pp. 100-107.
<https://doi.org/10.1016/j.powtec.2012.05.003>
53. T. B. Choe, P. Masse, A. Verdier, Membrane fouling in the ultrafiltration of polyelectrolyte solutions: Polyacrylic acid and bovine serum albumin, *J. Membr. Sci.* 26(1986) pp. 17-30.
[https://doi.org/10.1016/S0376-7388\(00\)80110-6](https://doi.org/10.1016/S0376-7388(00)80110-6)
54. F. B. Javier, A. L. Juan, A. I. Leal, and M. Gonzalez, The use of ultrafiltration and nanofiltration membranes for the purification of cork processing wastewater, *J. Hazard. Mater.* 162(2009) pp. 1438-1445.
<https://doi.org/10.1016/j.jhazmat.2008.06.036>